Available online at www.sciencedirect.com

SCIENCE DIRECT®

Developmental Biology 278 (2005) 336–346

DEVELOPMENTAL BIOLOGY

www.elsevier.com/locate/ydbio

Patterns of myocardial histogenesis as revealed by mouse chimeras

Daniel Eberhard, Harald Jockusch*

Developmental Biology and Molecular Pathology, Bielefeld University, W7 D-33501 Bielefeld, Germany

Received for publication 15 June 2004, revised 13 October 2004, accepted 9 November 2004
Available online 17 December 2004

Abstract

In order to study the pattern of clonal myocyte distribution during mammalian heart development, we have exploited embryo aggregation chimeras using, as cellular markers, an enhanced jellyfish green fluorescent protein (eGFP) transgene and a desmin-promoter-driven, nuclear-localized β-galactosidase (nlacZ) knock-in. In neonatal, weanling, and adult chimeric atria and ventricles, irregularly formed patches of various sizes rather than highly dispersed cardiomyocytes were observed. Most of the smaller patches and single cardiomyocytes were found in spatial neighborhood of large patches. This indicated largely coherent clonal growth during myocardial histogenesis combined with tangential displacement or active migration of myocytes. The patterns of ventricular walls were simpler than those of the septum and the atria. In the adult heart, large myocardial volumes devoid of eGFP-positive cardiomyocytes indicated a lack of secondary immigration of blood-borne stem cells into the myocardium. The patterns of oligoclonal expansions revealed in this work might be helpful in detecting and analyzing cell-lineage-based pathological processes in the heart.

Keywords: 3D reconstruction; Cell marking; Cell labeling; Clone; eGFP; Heart development; Mouse chimera; Myocardium; nLacZ; Patches

Introduction

Organogenesis of the vertebrate heart involves formation and revolution of the heart tube, regionalization into ventricles and atria, and growth, that is, extension and thickening of the walls by cell proliferation and postnatal hypertrophy (reviewed by Sedmera et al., 2000). A number of recent studies have dealt with the basic morphogenetic events in different regions of the developing vertebrate heart, like proliferation (Rychter et al., 1979; Soonpaa et al., 1996), apoptosis (Fisher et al., 2000), and cell mingling (Meilhac et al., 2003; Mikawa et al., 1992a).

In the chick heart, expansion of cell clones during morphogenesis of the ventricular myocardial walls has been analyzed after infection, at chosen developmental stages, with a β-galactosidase expressing retroviral vector (Mikawa et al., 1992a,b). Myocytes formed oligoclonal, cone-shaped wall segments which, at the time of hatching, often extended through the entire thickness of the ventricular wall. These findings supported the hypothesis that the proliferating progeny of early cardiomyoblasts in the heart tube delaminate towards the endocardium and expand more centripetally than tangentially.

In the mouse, mosaics based on rare events of somatic recombination (Eloy-Trinquet and Nicolas, 2002; Eloy-Trinquet et al., 2000) have been used to study subclonal expansions initiated at stochastic time points. These revealed lineage relationships during cardiogenesis and the effect of oriented mitotic growth of cardiomyocytes on heart morphogenesis (Meilhac et al., 2003, 2004a,b).

According to these studies, myocardial cells undergo an initial dispersive phase till the heart loop stage, followed by coherent growth during ventricular wall histogenesis (Meilhac et al., 2003). On the basis of these studies, it has been estimated that atrial and ventricular myocardium together derive from 140 to 180 precursors (Meilhac et al., 2004b).

In contrast to the foregoing labeling techniques, in embryo aggregation and ES cell injection chimeras, the genetic label is present from the very beginning of

* Corresponding author. Fax: +49 521 106 5654.
E-mail address: h.jockusch@uni-bielefeld.de (H. Jockusch).

0012-1606/$ - see front matter © 2004 Elsevier Inc. All rights reserved.
doi:10.1016/j.ydbio.2004.11.015

embryogenesis, the morula–blastocyst transition. However, there is a stochastic element in embryo-aggregation chimeras as well: Although, by combining two 8-cell stages, the blastocyst as a whole represents a "balanced" 1:1 contribution of the two parental sources, the resulting individual may be "unbalanced" due to random sampling of a small number of cells from the inner cell mass giving rise to the embryo proper. Whereas rare recombination or infection events will often result in one or a few clones in an embryo, in a balanced aggregation chimera containing a proportion of 0.4 to 0.6 of labeled cells, clones and oligoclonal patches may coalesce and thus information on individual clones may be lost (West, 1975). To estimate numbers of founder clones, unbalanced chimeras with contributions of <0.2 of labeled clones are therefore more valuable as rare patches are likely to represent clones or small oligoclones. However, chimeras with any proportion of parental contributions yield information on coherence vs. dispersal during clonal growth and on orientation of clonal expansions, as these are extracted from the properties of the patch borders and are independent of the clonality of the patches.

To study spatial patterns underlying myocardial histogenesis we have analyzed aggregation chimeras of the mouse in which one or both partners carried transgenes that are highly expressed in muscle, eGFP (Eberhard and Jockusch, 2004; Ikawa et al., 1999; Okabe et al., 1997) and a β-galactosidase transgene with a nuclear localization signal (nLacZ) under the control of the desmin promoter (Jockusch and Voigt, 2003; Li et al., 1996). Patch patterns observed in serial sections of neonatal, weanling, and adult chimeras enable us to distinguish between different models of clonal expansion patterns during myocardial development. While this work was in progress (Eberhard et al., 2002), fluorescent protein labeled chimeric hearts have been produced to test for germ line transmission of embryonic stem cells containing of various GFP variants (Hadjantonakis et al., 2002). However, these have not been exploited to study heart morphogenesis in detail.

Material and methods

Transgenic mice and production of aggregation chimeras

The origin of the mouse strains used, the expression of transgenes, and the production of embryo aggregation chimeras has been described (Eberhard and Jockusch, 2004; Jockusch et al., 2003). Chimeric morulae or early blastocysts were transplanted into pseudopregnant CD1 female recipient mice according to the German law for the protection of animals with an approved permit by the local authorities. The parental eGFP contribution of the individual chimeras was estimated from coat chimerism (McLaren, 1976; West, 1999).

Preparation of tissues and histochemical analysis

Hearts of juvenile or adult chimeras (killed by cervical dislocation) and decapitated neonatal chimeric animals were injected with 4% formaldehyde (FA) prepared freshly from para-FA in calcium and magnesium-free phosphate buffered saline (CMF-PBS) and postfixed at 4°C for 24 h in FA CMF-PBS (eGFP↔0 chimeras in 4% FA; eGFP↔LacZ chimeras in 2% FA), followed by 24 h in CMF-PBS. They were subsequently shock-frozen in liquefied propane (−190°C) followed by liquid nitrogen.

Frozen sections (8–10 μm) were stained with Hoechst 33258 (Sigma B 2261) to visualize nuclei. nLacZ-positive sections were stained for β-galactosidase and embedded in Elvanol (10g Mowiol 4–88 + 40 ml PBS + 20 ml glycerol). Smooth muscle α-actin immunostaining was performed with a Cy3-conjugated monoclonal anti-smooth muscle α-actin antibody (Sigma, C-6198). Sections were stained for desmin with a monoclonal anti-desmin antibody (Dako, M076001-2) using an appropriate horseradish peroxidase-labeled second antibody (Sigma, A9044) which was developed with diaminobenzidine (DAB, Sigma, D5905). eGFP was stained using a polyclonal anti-GFP antibody (MBL, 598) and an anti-rabbit Cy3-conjugated secondary antibody (Dianova, 211-166-003).

Microscopy, documentation, and morphometry

Specimens were observed with a UV stereomicroscope (Leica, Fluo III) and a Zeiss Axiophot microscope, and documented with a Nikon Coolpix 990 digital camera. Images were assembled and processed with Photoshop 5.5 (Adobe Systems Incorporated).

For quantification of patch areas, images from transversal sections to the apical–basal axis from the central ventricular level of each chimera were photographed under equal illumination conditions and equal scale (1 pixel = 5μm^2). Irrelevant signals within ventricle chambers (valve tissue) and surrounding the sections were eliminated ("blackened"). Resulting images were finally transformed to gray scale, that is, each pixel was assigned a distinct gray value between 0, "black" and 255, "white" corresponding to the highest intensity of green fluorescence.

Morphometric quantifications were performed using the public domain software ImageJ (version 1.26) developed at the U.S. National Institute of Health and available in the internet at http://rsb.info.nih.gov/ij/. Threshold values were defined by assigning each pixel to eGFP labeled or unlabeled areas. Patch areas were determined automatically using the ImageJ particle analysis feature. Neighboring cardiomyocytes or patches, which were artifactually separated by gaps or large intercellular areas in the tissue, were linked non-automatically under visual control. Very small areas (<125 μm^2, which is smaller than single cross-sectioned cardiomyocytes), that is, presumed artifacts, were excluded from the analysis. Because the ImageJ particle

analysis feature does not automatically subtract areas of "holes" in patches (=eGFP-negative areas), areas from larger "holes" were subtracted manually. Small "holes", including small eGFP-negative patches or cardiomyocytes, tissue gaps and very small blood vessels, were not considered. The total section area was determined analogously using a lower threshold, defining tissue and non-tissue area, and the mean section area calculated.

For normalization, patch areas of each section were assigned to classes according to their fractional contribution to the mean cross-section area of each individual chimeric heart, that is, patch sizes were normalized to the total area of the section. Classes represented fraction sizes of 1/n where the *n*'s were integer powers of 2 (i.e., 1/2, 1/4, 1/8, etc.). The frequency distribution of all sections of a given individual was based on the averages of each class.

3D Reconstruction

Images used for reconstruction were registered with SEM Align (Fiala and Harris, 2001) and rendered with the VolumeJ plugin written for ImageJ (Abramoff and Viergever, 2002). Parameters used for reconstruction were: voxel size (1,1,5), gradient spectrum, ramp gray values from 1 to 176 using spectrum Look Up Table (LUT), central classifier, gray value 150; deviation 2.

Results

Validation of cellular labels

A useful cellular label to study normal development should be cell-autonomously expressed in all cells of the cell-type under study and be physiologically neutral, that is, it should not interfere with developmental specification and not exert pathogenic effects. In the eGFP transgenic mouse strain used here, the protein eGFP is highly concentrated in cardiomyocytes (Jockusch et al., 2003) in the adult heart, and no eGFP-negative cardiomyocytes have been detected (see Supplementary material). In neonates, eGFP expression was lower than in the adult myocytes but was still high enough to discriminate eGFP fluorescence from background auto-fluorescence. In some cases, an eGFP antibody staining was used to verify eGFP labeling. Thus, in chimeras, eGFP is a reliable marker of parental origin and eGFP-labeled cardiomyocytes can be clearly discriminated from other cell types. In the myocardium, smooth muscle cells, which are also eGFP-positive, are much smaller than cardiomyocytes and confined to the walls of blood vessels (see Supplementary material). Since the occurrence of a dilated cardiomyopathy had been reported for GFP transgenic mice (Huang et al., 2000), we have tested markers for pathological changes in the myocardium of the eGFP mice used in this study. The levels of mRNAs indicative of hypertrophy, atrial natriuretic factor and the transcription factor GATA4 (Friddle et al., 2000), were not elevated as measured by RT-PCR (not shown). Thus, it is very likely that the eGFP marker used in this study is neutral for cardiac development and function. Furthermore, there was no indication of altered cell behavior during development.

In the case of the nLacZ label (Li et al., 1996), the heterozygous condition of the corresponding desmin knockout is not known to have any pathological effects. As shown by immunostaining, cardiac and smooth muscle cells in all nLacZ-positive chimeras were uniformly desmin positive indicating a heterozygous condition of the nLacZ allele, and thus a phenotypic wild-type condition with respect to desmin.

Surface aspects of chimeric hearts reveal large patches

Three neonatal, two weanling, and three adult eGFP↔nLacZ and eGFP↔0 chimeras were analyzed in detail (Table 1). Upon inspection under the UV stereomicroscope, large patches of eGFP-positive myocardium with fuzzy contours were seen (Fig. 1). In the chimeric ventricular myocardium of one low eGFP chimera (0.2 eGFP, chimera 4), the smallest eGFP-positive region contained approximately 30 cardiomyocytes surrounded by what appeared to be single cardiomyocytes of the same phenotype (Fig. 2B, arrows), whereas large patches con-

Table 1
Aggregation chimeras analyzed in this study

Nr (code)	Parental strains	Age (days)	Score	eGFP-positive contribution	Score
1	C57Bl/6-eGFP↔129-nlacZ	2	neonate	~0.3[a]	low eGFP
2	C57Bl/6-eGFP↔129-nlacZ	2	neonate	~0.1[a]	low eGFP
3	C57Bl/6-eGFP↔CD1	4	neonate	~0.6[a]	balanced
4	C57Bl/6-eGFP↔CD1	21	weanling	~0.2[b]	low eGFP
5	C57Bl/6-eGFP↔CD1	23	weanling	~0.6[b]	balanced
6	C57Bl/6-eGFP↔CD1	57	adult	~0.5[b]	balanced
7	C57Bl/6-eGFP↔CD1	57	adult	~0.1[b]	low eGFP
8	C57Bl/6-eGFP↔CD1	81	adult	~0.6[b]	balanced

[a] As judged from eGFP-positive vs. -negative skin areas.
[b] As judged from black vs. albino coat color.

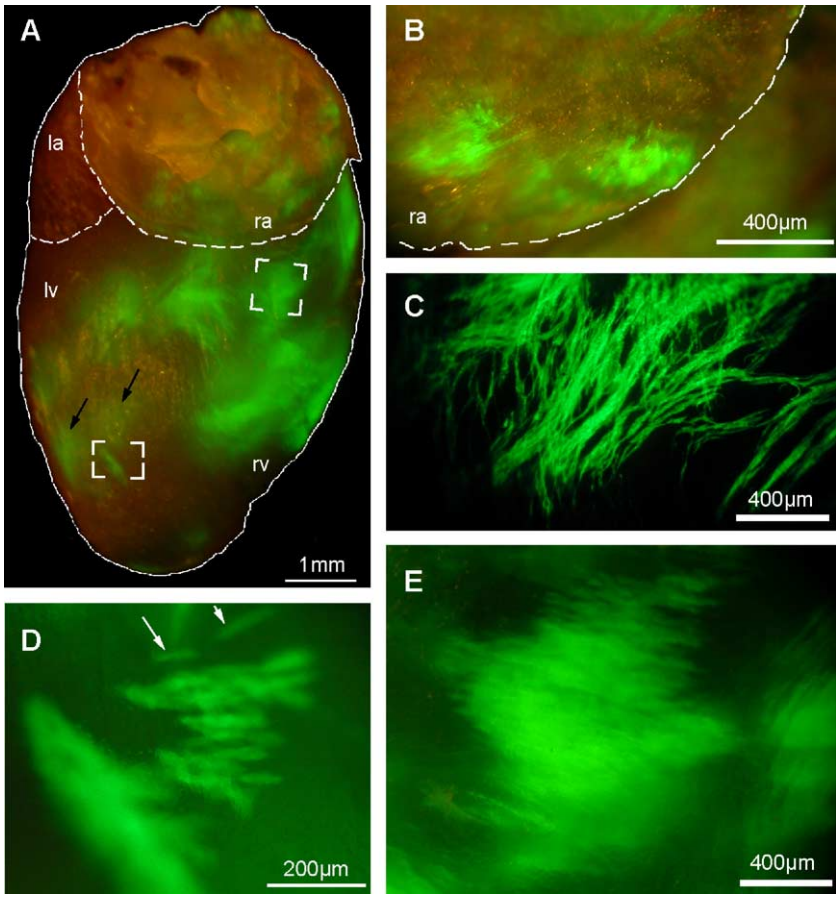

Fig. 1. Surface aspects of the heart of an unbalanced (0.2 eGFP) weanling eGFP↔0 chimera. (A) Under the UV stereomicroscope, eGFP-positive patches of various sizes are seen in the atrial and ventricular walls. Those with lower apparent fluorescence intensities (arrows) are localized in deeper layers. (B) Patches with fuzzy borders and (C) "bundles" of cardiomyocytes in the right atrial wall. (D, E) Enlargements of ventricular patches as framed in (A). (D) Small patch in the left ventricular wall, arrows point to single cardiomyocytes; (E) large patch in the right ventricular wall. (A, B) Illumination with UV and visible-light; (C, D, E) UV-light only, la, left atrium; lv, left ventricle; rv, right ventricle.

tained hundreds of cardiomyocytes and covered up to approximately 10% of the ventricular surface (Fig. 1E). Dispersed patterns of cardiomyocytes were exclusively observed at the borders of the eGFP patches in the ventricular myocardium (Figs. 1A, D, E), that is, isolated eGFP-labeled cardiomyocytes were not observed in the center of eGFP-negative areas and vice versa. At the surface of the atria, eGFP-labeled cardiomyocytes also appeared in patches rather than dispersed (Figs. 1B, C). Atrial cardiomyocytes had a more elongated, rather fibrous shape compared to ventricular myocytes (Fig. 1C).

Fluorescence-stereomicroscopic observation showed that some large eGFP patches extended into the depth of ventricular walls, thus, representing more or less solid 3-dimensional structures, but did not allow one to discriminate whether these were free of small groups of non-labeled cardiomyocytes.

Patches and dispersed myocytes in the ventricular walls

To analyze the spatial distribution of labeled cardiomyocytes at high resolution, chimeric hearts were serially sectioned. In larger patches of neonatal nLacZ↔eGFP chimeric hearts, the two labels were mutually exclusive and there were no myocytes devoid of either label (Figs. 2A, A′). However, in some regions, the two labels seemed to be interspersed (Figs. 2B, B′).

Cross-sections through ventricular walls revealed large regions of eGFP-positive patches and small patches or single cardiomyocytes which either surrounded large patches or appeared in clusters, that is, they were non-randomly distributed (Fig. 2). All large patches had fuzzy outlines, that is, there was intermingling of eGFP-positive and -negative cardiomyocytes at their borders, and appeared interspersed with cardiomyocytes of the other parental type, as in the myocardium of neonatal nLacZ↔eGFP chimeras, which contained large eGFP patches embedding nLacZ-positive cardiomyocytes (Figs. 2B, B′, arrows), or in a weanling (Fig. 2C) and adult eGFP↔0 chimera (Figs. 2D–F′).

Although in each chimera there were some large patches which extended through the whole thickness of ventricular walls (Figs. 2A, A′, D, E), in most cases, the patches were non-transmural and appeared as staggered

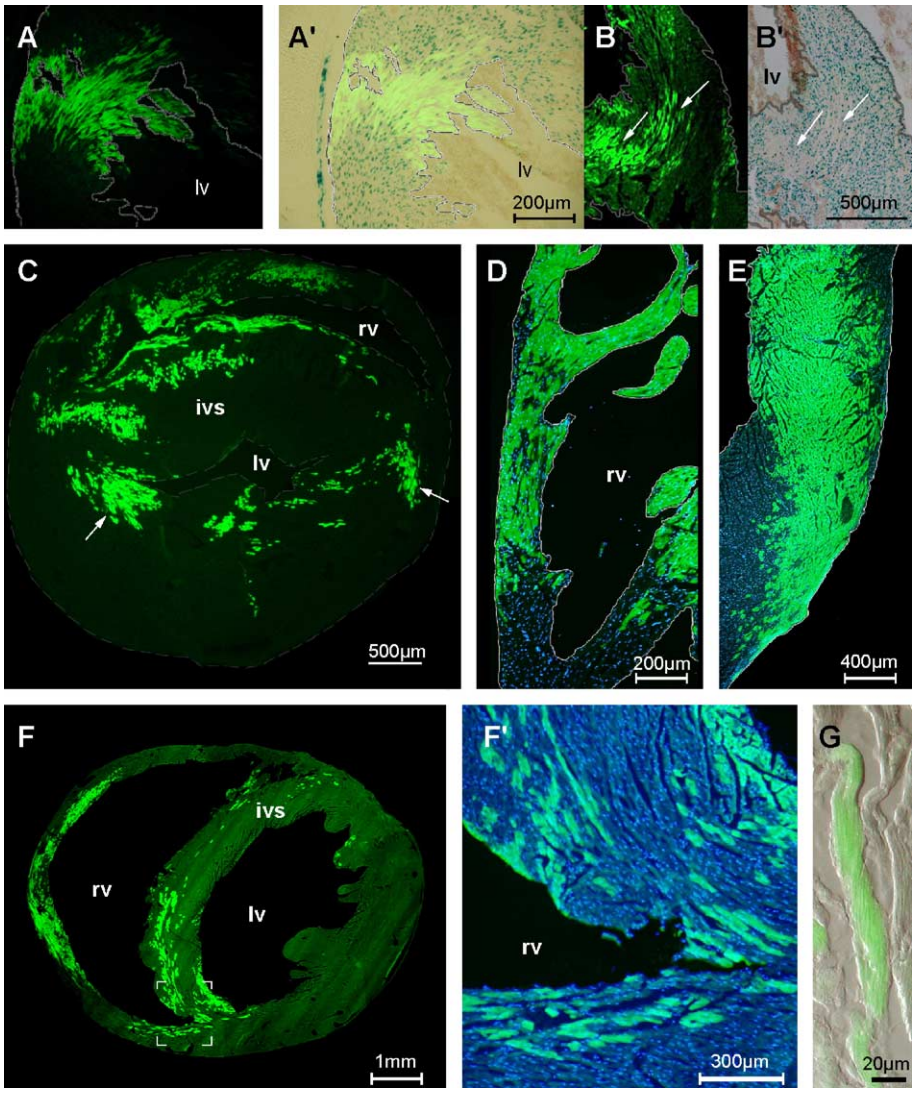

Fig. 2. Sections of patches in the ventricular chimeric myocardium. (A–B′) Transverse section through the ventricle of a low eGFP neonatal nLacZ↔eGFP chimera. eGFP-positive and nLacZ-positive regions are mutually exclusive at some places (nLacZ-negative transmural patch in left neonatal ventricular wall, A, A′), interspersed at others (B, B′, arrows). (C) Transverse section at ventricular level of a heart of an unbalanced eGFP↔0 chimera (0.2 eGFP) with non-transmural eGFP patches and large eGFP-negative areas in the left ventricular wall. (D, E) Longitudinal sections through ventricle walls of an adult balanced chimera. (D) Patch in the right ventricular wall with pure eGFP-positive (upper) and mixed (lower) trabeculae. (E) Large transmural eGFP-positive patch. (F, F′) Transverse section through ventricles of an adult low eGFP chimera showing large patches in the left, as well sparse but clustered small patches in interventricular septum and in the left ventricle. (F′) Enlargement of the junction of interventricular septum and right ventricular wall as framed in (F). (G) Enlargement of eGFP-positive cardiomyocytes typically seen near the margins of large patches of like phenotype. (A, B, C, F) eGFP fluorescence combined with Hoechst overlay to show all nuclei in (D′, E, F). (A′) bright field to show nLacZ-positive nuclei; (B′) Overlay of fluorescence and bright field; (G) Overlay of eGFP fluorescence and Nomarski contrast. A–B′, Drawn lines, outline of ventricular walls; left ventricle; rv, right ventricle; ivs, interventricular septum.

tangentially orientated groups of cardiomyocytes of alternating phenotype that extended through the myocardial wall (Fig. 2C, arrow).

As expected, patches in balanced chimeras were larger than in low eGFP chimeras (see below) reflecting random coalescence of clones with the same label (cf. West, 1975). The ventricular myocardium of the low eGFP chimeras contained large eGFP-free regions (Figs. 2C, F).

Large patches appeared in left and right ventricular wall. Extensions of eGFP patch clusters from the left to the right ventricular wall were minimal indicating a compartment border. Rather, patches frequently extended from the left ventricle into the interventricular septum following the fiber orientation (e.g., Figs. 2F, F′ and 4A, B). In the interventricular septum, eGFP patches extended for much smaller distances along the basal–apical axis than in the ventricular walls. Even in chimeras with low parental eGFP contributions, many eGFP-positive patches were observed in one section of the interventricular septum, indicating intermingling during the formation of the septum.

Clustered eGFP-labeled cardiomyocytes in the atrium

In sections, the atrial walls of neonates, weanling (not shown) and adult (Fig. 3) chimeras predominantly consisted of small eGFP-positive patches and clusters of eGFP-labeled cardiomyocytes (Fig. 3A, arrows, Fig. 3B) indicating that they derive from larger patches. Such large patches of eGFP-positive were observable in the folded atrial walls; the folds were never exclusively eGFP-positive or -negative, indicating their oligoclonal origin (Fig. 3A′).

3D evaluation of patches

To verify the presence of single eGFP-positive cardiomyocytes within a solid tissue environment derived from the other parental origin (see Figs. 1D and 2G), that is, to exclude that "one-cell patches" merely represent the tips of larger patches, the central part of the ventricle of an adult balanced chimera was reconstructed in 3D from serial sections. The reconstruction revealed large, nearly eGFP-free regions in the left and right ventricular wall, which can be traced deep into the myocardium (Figs. 4C, C′, see movie 1 in supplement). Within these areas, single eGFP-positive cardiomyocytes (Fig. 3D) and small patches (Figs. 4C, C′) are present. When following patches through the serial sections in axial direction, one gets the impression of a rotating streaming movement (supplement, movie 2). Thus, the direction, along which myocardial cell clones extend, reflects the longitudinal orientation of myocytes in the adult heart. This observation is consistent with results of retroviral labeling experiments in chick (Mikawa et al., 1992a).

Patch size distributions do not depend on postnatal age

Areas of 10,806 patches in 20 transverse sections from the central ventricular level of six chimeras (of each stage, neonatal, weanling, and adult, one balanced and one unbalanced) were determined and expressed as fractions

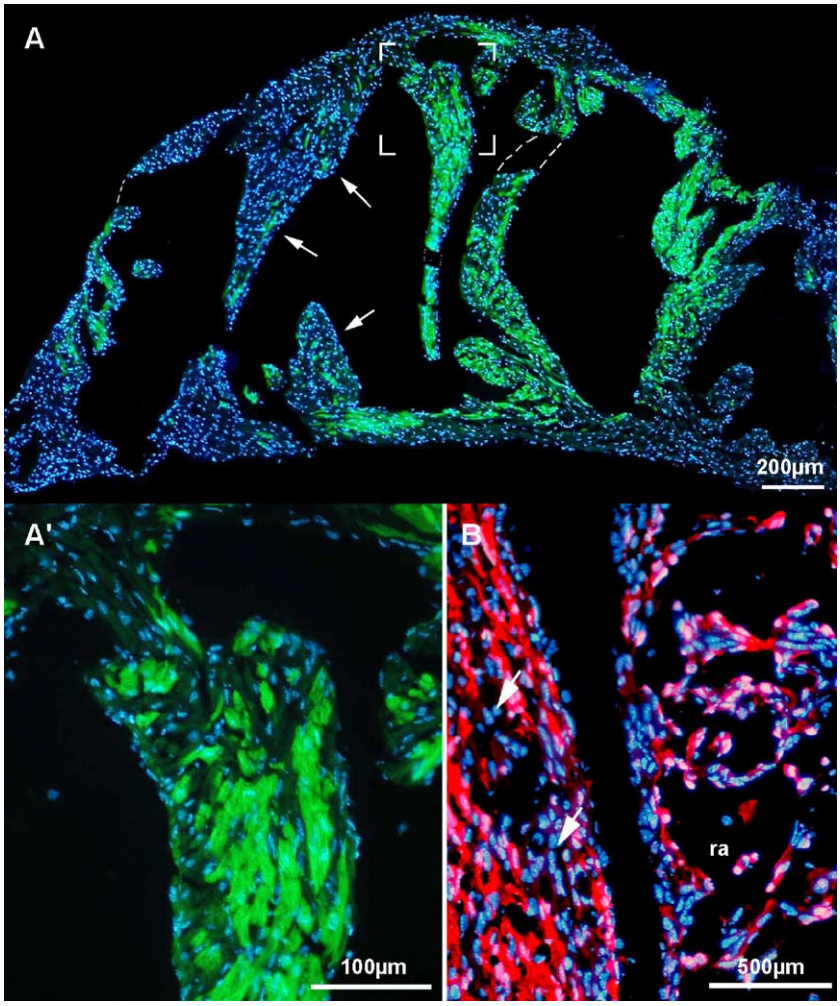

Fig. 3. Internal organization of patches in chimeric atria. (A) eGFP-positive patches and single cardiomyocytes (arrows) and larger patches in adult atrial walls; (A′) enlargement as framed in (A), showing the patch structure in at single cell resolution. (B) eGFP immunostaining of section of a balanced neonatal eGFP↔0 chimera revealing small interspersed eGFP-negative regions (arrows) in the right ventricle and eGFP-positive clusters of cardiomyocytes in the atrial folds and walls. (A, A′), Merge of eGFP fluorescence and Hoechst nuclear stain. (B), Overlay of anti-eGFP staining and Hoechst nuclear stain; ra, right atrium.

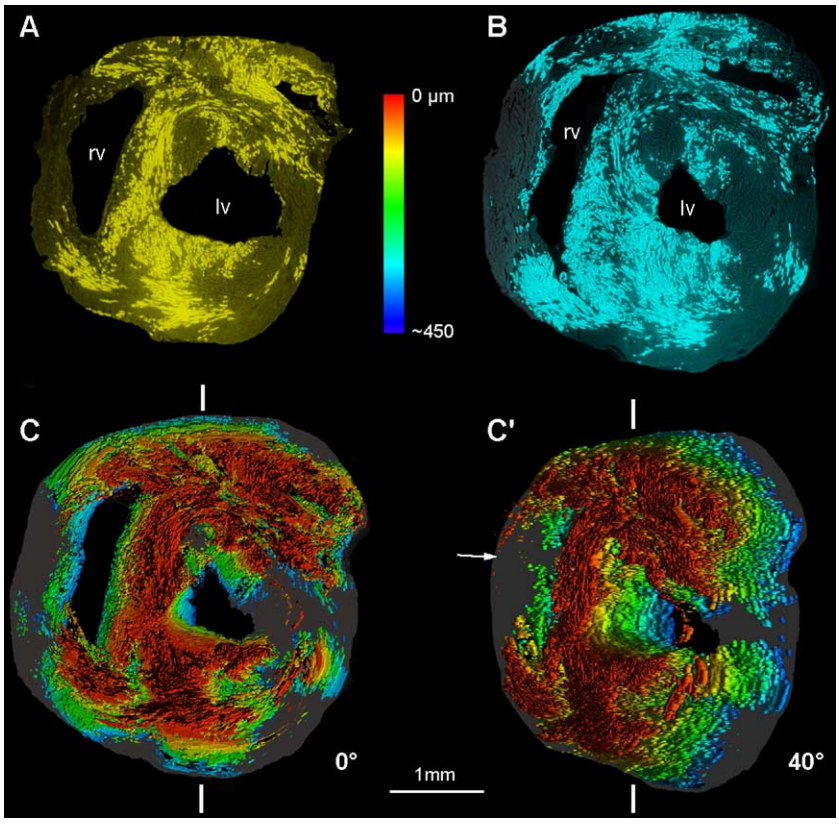

Fig. 4. Reconstruction of a central ventricular segment (thickness approximately 450 µm) of a balanced eGFP↔0 chimera. (A, B) Examples of transversal sections at level approximately 100 and 300 µm used for reconstruction with eGFP-positive areas color-coded for relative depth from basal to apical as indicated by color scale. (C, C′) 3D reconstruction using 24 levels. (C) 3D view from heart base of eGFP-positive areas in registered stack of images with color code for depth as in color scale. Due to the overlapping of the eGFP patches of single sections, not all of the eGFP-free regions inside the reconstructed segment can be seen. Gray, non-eGFP tissue. (C′) Stack rotated by 40° around vertical axis deleted. For clarity, valves are not shown. For animated rotation, see movie 1; for the displacement of patches as a function of depth, see movie 2 in supplementary material.

of the total area of the section. By this normalization, age-dependent size differences of the hearts were largely eliminated. Due to the different angles of cardiomyocyte orientation (and thereby varying cross-sectional areas) and variation due to tissue shrinkage, patch areas cannot be easily converted into numbers of cardiomyocytes. Patch size distributions were surprisingly similar in all chimeras, indicating little variation of the pattern with age (Fig. 5A). As expected, patches in balanced chimeras were larger than in unbalanced of the same age.

Spatial distribution of small patches is non-random

"Small patches" in sections may either derive from small 3D patches or represent sections of extensions of larger 3D patches. In order to find out any regularities in the spatial distribution of small patches, we measured their density as a function of their distance to the nearest large patch. Rather than being scattered in a random fashion, their density declined with the distance from the nearest large patch, and usually declined to zero at distances of approximately 300 µm, leaving large parts of the ventricular wall completely free of eGFP cells. Thus, even truly small 3D patches were clearly in association with large patches (Fig. 5B). The converse must be true for non-labeled, eGFP-negative patches but this is technically more difficult to demonstrate.

Discussion

Principles of the retrospective analysis of chimeras

The following principles must underlie any inference from chimeric patterns on developmental processes:

(1) The principle of equivalence and complementarity. Any statement referring to labeled cells in a label↔non-label chimera should likewise be true for unlabeled cells. This follows from the postulate that the label should be physiologically neutral, that is, does not affect developmental specification and growth rate. The different aspect of labeled vs. unlabeled clones or the technical advantage of low eGFP vs. low non-eGFP chimeras is thus only a matter of the analytical methods employed.

(2) The principle of "cellular entropy". From the developmental equivalence of labeled and non-labeled cells, it follows that any dispersion of one kind within the

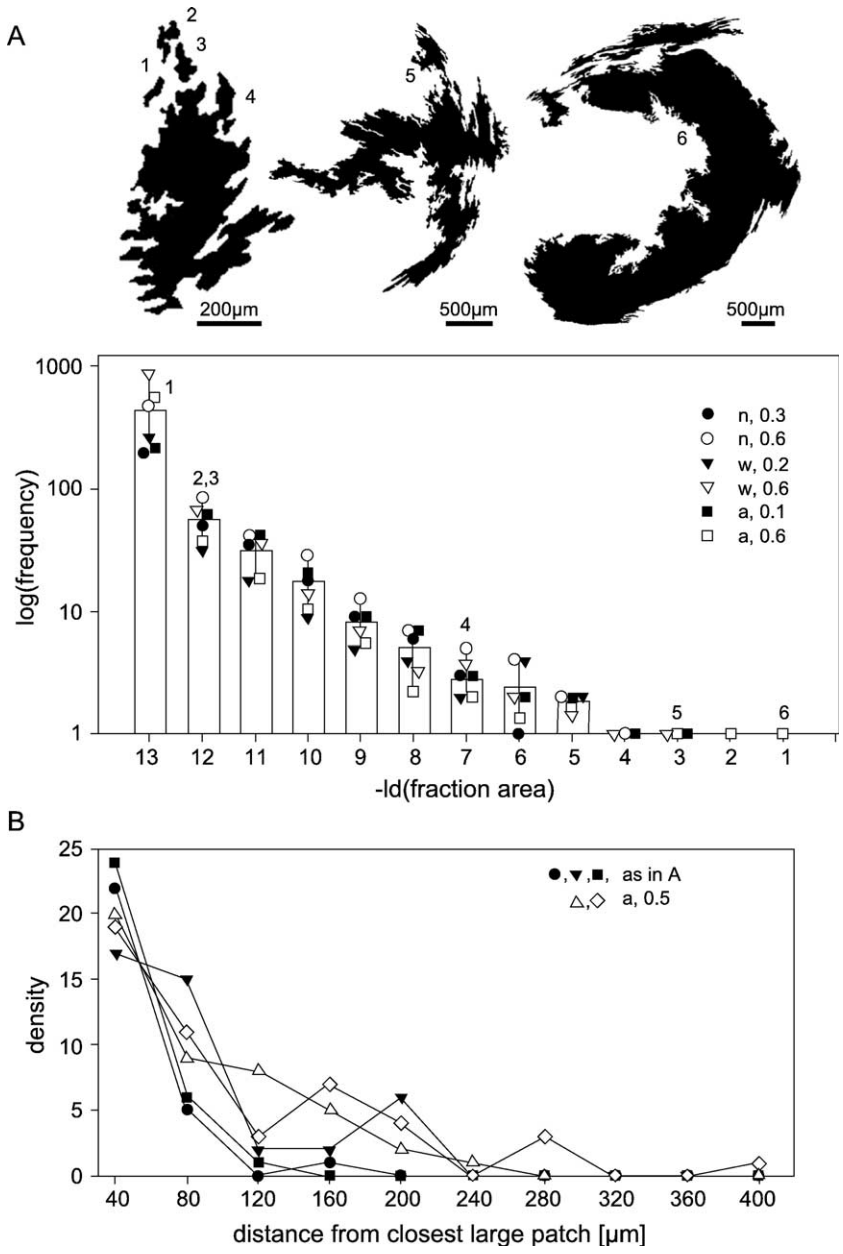

Fig. 5. Quantification of patch areas and spatial distribution in chimeric ventricles. (A) Upper panel: examples of patches used for quantification of areas. Numbers refer to size classes in lower panel. Lower panel: frequency distributions of patch areas, for different age groups and parental contributions. Abscissa, classes represent patch sizes as fractions of section areas, expressed as $1/n$ where the n's are integer powers of 2 (i.e., 1/2, 1/4, 1/8 etc.); −ld, negative logarithmus dualis. Ordinate, frequency = number of patches in each class. Solid symbols indicate unbalanced, empty symbols balanced chimeras. Each symbol represents an average from four (two in neonates) sections from the central part of a chimeric ventricle. Column heights are means. Numbers indicate classes from which the sample patches 1–6 are shown in the upper panel. Patch 6 is the largest patch observed (0.38 contribution to the total section area). Abbreviations: n, neonatal, w, weanling, a, adult, decimal fractions are eGFP contributions of the respective chimeras. (B) Densities of eGFP-labeled cardiomyocytes and small patches as a function of the distance to nearest large patch. eGFP-positive cardiomyocytes and small patches in segments (40 µm width) surrounding the border of the closest large patch were counted.

other or intermingling of two kinds would not reverse. Thus, if highly dispersed patterns are seen at an early but coherent patterns at a later stage of organogenesis, this can only come about by a few clones (irrespectively of their labeling phenotype) overgrowing all others, or a founder effect, that is, a small number of clones settling in an unoccupied niche and expanding (cf. Eberhard and Jockusch, 2004).

(3) The 3D nature of most tissues must be taken into account. Many chimera analyses have been performed on epithelia where the developmental history can be completely visualized in two dimensions (West, 1999). In solid tissues, expansion of clones occurs in three dimensions of which 2D sections can only give an incomplete representation, for example, a "small patch" next to a large patch may actually be an

extension of the large patch, as 3D reconstruction of serial sections will reveal. Furthermore, coalescence of clones or patches is much more extensive in three than in two dimensions (cf. West, 1975).

Low variability and age independence of patch patterns

Our previous analysis of skeletal muscle chimerism (using the same set of chimeras, Eberhard and Jockusch, 2004) has revealed vast inter-individual differences. Some chimeras were more homogeneous, others showed drastic left–right differences in back muscles or differences between large muscles or muscle groups in limbs. In contrast, the patch size distribution in chimeric hearts was reproducible from individual to individual. Furthermore, there was no dependence on postnatal age. This indicates that postnatal growth does not alter the clonal patterns that have arisen during organogenesis. This is consistent with the notion that mitotic activity of cardiomyocytes decreases drastically during late fetal development of the mouse (Soonpaa et al., 1996). Thus, major changes of the initial neonatal patch morphology and size presumably result from hypertrophy (Claycomb, 1977) and limited changes in myocyte orientation (McLean and Prothero, 1991). Apoptosis (Fernandez et al., 2001) and cell mingling are of minor significance during postnatal growth. The shapes of patches, their staggering in the depth of ventricular walls, and their fuzzy margins suggest that displacement from large patches is not random. Rather, it seems more extensive in the longitudinal direction of cardiomyocytes thus coinciding with the direction of contractile force, and the layers of a clone may show a less firm adherence in the radial direction so that tangential "slippage" may occur; this would explain the distribution of clonally derived myocyte layers in tangentially orientated groups of cardiomyocytes. The connection of myocytes by intercalated discs, as a response to mechanical stress, may restrict myocyte motility. In regenerating myocardium, cardiomyocyte may revert to a more motile status (Jockusch and Heimann, 1991).

Atria and interventricular septum compared to ventricular walls

There were some extended patches in the atrial walls but the general patterns seemed to be more dispersed than those of the ventricles, indicating either a higher number of founder clones (despite the much smaller mass of the mature organ) or more dispersive growth patterns or both.

In the interventricular septum, a complex patch pattern is generated due to the stretching during growth by the surrounding ventricular walls (Rychter et al., 1979). Thus, many subclones may contribute during the process of axial elongation of the septum. This is consistent with the observation of patches with a wide variability of sizes even in low eGFP chimeras. Radial extension of clones has been proposed to be the basis of the development of the interventricular septum in chick (Mikawa and Fischman, 1996).

Models for myocardial histogenesis and number of progenitors

Considering the theorems outlined above, the retrospective interpretation of chimeric patch patterns in terms of clonal behavior underlies certain restrictions. Possible pathways leading to different patch patterns in a mature chimeric heart are shown in Fig. 6. This model considers four mechanisms of possible importance for the clonal distribution of cardiomyocytes in the mature heart. The important parameters are (a) number of progenitors (tens to hundreds vs. thousands), (b) the degree of intermingling due to movements of cardiomyocytes within the developing tissue (no movement corresponds to ideal coherent expansion); (c) loss of clones; (d) the occurrence of secondary immigration of blood-borne stem cells into the myocardium.

A highly dispersed pattern of clonal origins of cardiomyocytes in the mature heart might either be due to a large number of progenitors or a high degree of intermingling. The extreme results would be a limited number of large patches with well-defined borders (Fig. 6I) or a highly dispersed pattern (Fig. 6III). The first pattern would be most easily explained by a small (tens) or moderate (hundreds) numbers of progenitor cells giving rise to clones that expand in a coherent fashion, whereas the latter could come about by either a very large number (thousands) of progenitor cells, or extensive intermingling or a combination of both. Although, according to the cellular entropy theorem, intermingling cannot be reversed, a pattern of large patches could still arise if the majority of clones was lost at an intermediate developmental stage, either due to cell death or by proliferation rates being by orders of magnitude lower than those of the "fittest" clones. At least for the period between embryonic days 8.5 and 10.5 extensive loss of that kind has been excluded (Meilhac et al., 2003).

Our patch patterns (Fig. 6II) are intermediate between I and III indicating largely coherent growth of a limited number of progenitors (and/or a reduction of the number of progenitor clones) with limited myocyte displacement and intermingling: There are mini-patches and even single cardiomyocytes in the proximity of large patches as shown by quantitative evaluation. The spatial distribution of these small elements is not random in that they are usually associated with larger patches. This type of intermingling may either be due to short-distance active migration of cardiomyocytes, or to passive displacement due to "squeezing" caused by the continuous contractions of the tissue during its development, or both. The alternative explanation that the dispersed mini-patches

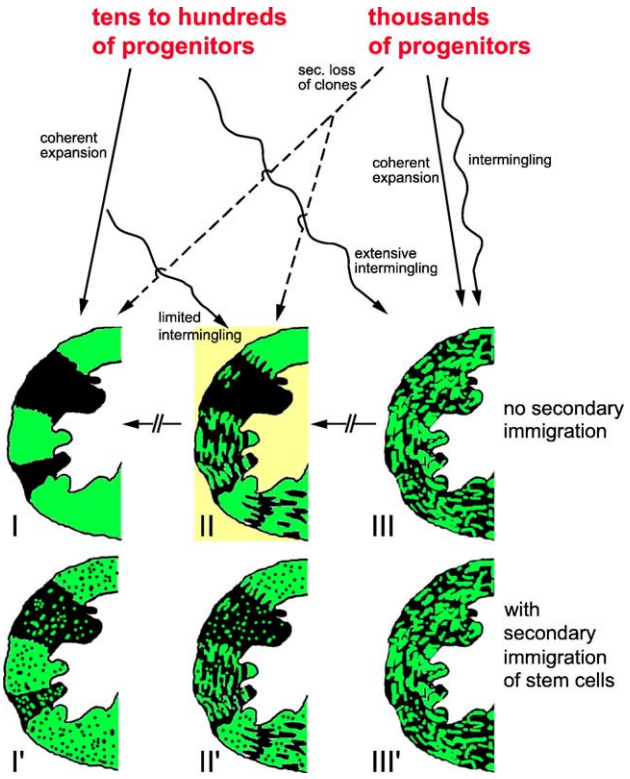

Fig. 6. Models for the relationship between modes of clonal expansion and chimeric patch patterns in the myocardium. Straight arrows indicate coherent expansion of clones, wiggly arrows indicate dispersal and intermingling. Dashed arrows indicate extensive loss of cardiomyocytes or cardiomyocyte clones. Shown are patch patterns of ventricular walls: I, small number of large patches with distinct borders; III, dispersed pattern; II, intermediate pattern: irregular patches of different sizes with rugged borders. These patterns depend on the sizes of progenitor pools and the relative contribution of intermingling and coherent expansion. Coherent patterns cannot arise from dispersed patterns (interrupted arrows) except, in an early phase of growth, by loss of clones (dashed arrows) or founder effects in niches of expansion, for example, at the tips of trabeculae. Secondary formation of cardiomyocytes from blood-borne stem cells would lead to interspersed myocytes within otherwise coherent areas of the alternative parental phenotype, as shown in I′ and II′, but would not be visible in a genuinely dispersed pattern (III′). The patch pattern observed in this work corresponds to II: there are patches of varying sizes with fuzzy outlines and even single myocytes in the proximity of large patches. This argues for largely coherent growth of a limited number of progenitors (and/or a reduction of the number of progenitor clones) with limited myocyte displacement and intermingling. There was no indication for secondary stem cell immigration.

and single myocytes represent independent clones with a zero or low proliferation rate seems excluded by their preferential occurrence in the neighborhood of large patches.

From grafting experiments in early mouse embryos, it was concluded that about 50 cells of the epiblast are allocated to the heart mesoderm (Tam et al., 1997). Independently, the number of progenitor cells, for example, for the ventricular walls, can be roughly estimated from chimeric patch patterns. In deriving sizes and numbers of clones from patch patterns, coalescence would lead to an overestimate of sizes and an underestimate of numbers, whereas splitting of clones would have the opposite effect. The probability of coalescence of clones is minimized in chimeras with a low contribution by the labeled partner. In a low eGFP chimera (number 4 in Table 1; approximately 0.2 eGFP as judged by coat color) about 20 medium sized and large patches were discriminated in the ventricle. As estimated from serial sections, these comprised approximately 1/6 of the volume. The number of progenitors of the ventricular myocardium could thus be estimated as $6 \times 20 = 120$. This would be somewhat higher but not too far from the estimate for the founder pool for the whole myocardium of 140–180 cells based on somatic recombination (Meilhac et al., 2004a).

Absence of secondary immigration of stem cells into the mature myocardium

Secondary immigration of stem cells which turn into cardiomyocytes has been claimed to occur in human heart transplants (Quaini et al., 2002) raising the possibility of immigration of stem cells, for example, from the hematopoietic system, as a contribution to normal tissue turnover of the myocardium. A secondary immigration of stem cells via the blood vessels should lead to a dispersed distribution (Figs. 6I′, II′, III′), perhaps with accumulations close to capillaries. According to this criterion, a contribution of $\geq$5% of cardiomyocytes by immigrant stem cells can be excluded since single cardiomyocytes or miniclones distributed independently of patches were not observed at a resolution of single labeled cardiomyocytes. Thus, “late comers”, that is, an influx of stem cells via blood vessel after cardiac organogenesis did not significantly contribute to the mass of the myocardium of the mice studied in this work. This does not exclude that secondary immigration of cardiac stem cells might occur after pathological insult to the myocardium, for example, after heart transplantation (Quaini et al., 2002). However, the observations on patients are still controversial, especially with respect to the cardiomyocyte nature of the immigrant cells (Glaser et al., 2002).

Conclusion

The present chimera analysis has revealed, in the postnatal mouse heart, patterns of parental contributions that are best explained by a coherent clonal expansion and a limited dispersal of myocytes. Although the specific patterns are stochastic in nature, there was a remarkable overall similarity of patterns between individuals and no systematic variation with postnatal age. The clonal patterns were more complicated in atria and in the septum than in the ventricular walls. We assume that similar patterns hold for the human heart. Cell-lineage related pathological phenotypes may therefore occur in patch patterns similar to those shown in the mouse model.

Acknowledgments

We thank Professors Masaru Okabe (Osaka University) for providing the eGFP transgenic mouse strain, Dr. Volker Schmidt (now Physiological Institute, Medical Faculty, Würzburg University), and Sandra Heising for help with embryological techniques. This work was supported by the Deutsche Forschungsgemeinschaft (DFG), Graduate Program 231 "Strukturbildungsprozesse" and by Fonds der Chemischen Industrie.

Appendix A. Supplementary data

Supplementary data associated with this article can be found, in the online version, at doi:10.1016/j.ydbio.2004.11.015.

References

Abramoff, M.D., Viergever, M.A., 2002. Computation and visualization of three-dimensional soft tissue motion in the orbit. IEEE Trans. Med. Imag. 21, 296–304.

Claycomb, W.C., 1977. Cardiac-muscle hypertrophy. Differentiation and growth of the heart cell during development. Biochem. J. 168, 599–601.

Eberhard, D., Jockusch, H., 2004. Intermingling versus clonal coherence during skeletal muscle development: Mosaicism in eGFP/nLacZ-labeled mouse chimeras. Dev. Dyn. 230, 69–78.

Eberhard, D., Voigt, S., Jockusch, H., 2002. Patterns of muscular organogenesis and stem cell migration as revealed by lacZ/GFP double-labelled mouse chimeras. J. Muscle Res. Cell Motil. 23, 175–186.

Eloy-Trinquet, S., Nicolas, J.F., 2002. Clonal separation and regionalisation during formation of the medial and lateral myotomes in the mouse embryo. Development 129, 111–122.

Eloy-Trinquet, S., Mathis, L., Nicolas, J.F., 2000. Retrospective tracing of the developmental lineage of the mouse myotome. Curr. Top. Dev. Biol. 47, 33–80.

Fernandez, E., Siddiquee, Z., Shohet, R.V., 2001. Apoptosis and proliferation in the neonatal murine heart. Dev. Dyn. 221, 302–310.

Fiala, J.C., Harris, K.M., 2001. Extending unbiased stereology of brain ultrastructure to three-dimensional volumes. J. Am. Med. Inform. Assoc. 8, 1–16.

Fisher, S.A., Langille, B.L., Srivastava, D., 2000. Apoptosis during cardiovascular development. Circ. Res. 87, 856–864.

Friddle, C.J., Koga, T., Rubin, E.M., Bristow, J., 2000. Expression profiling reveals distinct sets of genes altered during induction and regression of cardiac hypertrophy. Proc. Natl. Acad. Sci. U. S. A. 97, 6745–6750.

Glaser, R., Lu, M.M., Narula, N., Epstein, J.A., 2002. Smooth muscle cells, but not myocytes, of host origin in transplanted human hearts. Circulation 106, 17–19.

Hadjantonakis, A.K., Macmaster, S., Nagy, A., 2002. Embryonic stem cells and mice expressing different GFP variants for multiple non-invasive reporter usage within a single animal. BMC Biotechnol. 2, 11.

Huang, W.Y., Aramburu, J., Douglas, P.S., Izumo, S., 2000. Transgenic expression of green fluorescence protein can cause dilated cardiomyopathy. Nat. Med. 6, 482–483.

Ikawa, M., Yamada, S., Nakanishi, T., Okabe, M., 1999. Green fluorescent protein (GFP) as a vital marker in mammals. Curr. Top. Dev. Biol. 44, 1–20.

Jockusch, H., Heimann, P., 1991. Morphological self-organization and functional activity of ectopically grafted atrial tissue. In: Oberpriller, J.O., Oberpriller, J.C., Mauro, A. (Eds.), The Development and Regenerative Potential of Cardiac Muscle. Harwood Academic Publishers, London, pp. 139–155.

Jockusch, H., Voigt, S., 2003. Migration of adult myogenic stem cells as revealed by GFP/nLacZ transgene labeling and muscle transplantation in the mouse. J. Cell Sci. 116, 1611–1616.

Jockusch, H., Voigt, S., Eberhard, D., 2003. Localization of GFP in Frozen Sections from Unfixed Mouse Tissues. Immobilization of a highly soluble marker protein by formaldehyde vapor. J. Histochem. Cytochem. 51, 401–404.

Li, Z., Colucci-Guyon, E., Pincon-Raymond, M., Mericskay, M., Pournin, S., Paulin, D., Babinet, C., 1996. Cardiovascular lesions and skeletal myopathy in mice lacking desmin. Dev. Biol. 175, 362–366.

McLaren, A., 1976. Mammalian chimaeras. Cambridge University Press, Cambridge.

McLean, M., Prothero, J., 1991. Myofiber orientation in the weanling mouse heart. Am. J. Anat. 192, 425–441.

Meilhac, S.M., Kelly, R.G., Rocancourt, D., Eloy-Trinquet, S., Nicolas, J.F., Buckingham, M.E., 2003. A retrospective clonal analysis of the myocardium reveals two phases of clonal growth in the developing mouse heart. Development 130, 3877–3889.

Meilhac, S.M., Esner, M., Kelly, R.G., Nicolas, J.F., Buckingham, M.E., 2004a. The clonal origin of myocardial cells in different regions of the embryonic mouse heart. Dev. Cell 6, 685–698.

Meilhac, S.M., Esner, M., Kerszberg, M., Moss, J.E., Buckingham, M.E., 2004b. Oriented clonal cell growth in the developing mouse myocardium underlies cardiac morphogenesis. J. Cell Biol. 164, 97–109.

Mikawa, T., Fischman, D.A., 1996. The polyclonal origin of myocyte lineages. Annu. Rev. Physiol. 58, 509–521.

Mikawa, T., Borisov, A., Brown, A.M., Fischman, D.A., 1992a. Clonal analysis of cardiac morphogenesis in the chicken embryo using a replication-defective retrovirus: I. Formation of the ventricular myocardium. Dev. Dyn. 193, 11–23.

Mikawa, T., Cohen-Gould, L., Fischman, D.A., 1992b. Clonal analysis of cardiac morphogenesis in the chicken embryo using a replication-defective retrovirus: III. polyclonal origin of adjacent ventricular myocytes. Dev. Dyn. 195, 133–141.

Okabe, M., Ikawa, M., Kominami, K., Nakanishi, T., Nishimune, Y., 1997. 'Green mice' as a source of ubiquitous green cells. FEBS Lett. 407, 313–319.

Quaini, F., Urbanek, K., Beltrami, A.P., Finato, N., Beltrami, C.A., Nadal-Ginard, B., Kajstura, J., Leri, A., Anversa, P., 2002. Chimerism of the transplanted heart. N. Engl. J. Med. 346, 5–15.

Rychter, Z., Rychterova, V., Lemez, L., 1979. Formation of the heart loop and proliferation structure of its wall as a base for ventricular septation. Herz 4, 86–90.

Sedmera, D., Pexieder, T., Vuillemin, M., Thompson, R.P., Anderson, R.H., 2000. Developmental patterning of the myocardium. Anat. Rec. 258, 319–337.

Soonpaa, M.H., Kim, K.K., Pajak, L., Franklin, M., Field, L.J., 1996. Cardiomyocyte DNA synthesis and binucleation during murine development. Am. J. Physiol. 271, 2183–2189.

Tam, P.P., Parameswaran, M., Kinder, S.J., Weinberger, R.P., 1997. The allocation of epiblast cells to the embryonic heart and other mesodermal lineages: the role of ingression and tissue movement during gastrulation. Development 124, 1631–1642.

West, J.D., 1975. A theoretical approach to the relation between patch size and clone size in chimaeric tissue. J. Theor. Biol. 50, 153–160.

West, J.D., 1999. Insights into development and genetics from mouse chimeras. Curr. Top. Dev. Biol. 44, 21–66.